Admittance spectroscopy of $Si/Si_{1-x}Ge_x/Si$ quantum well systems: Experiment and theory

Xi Li,[1] W. Xu,[2,3,*] FengYing Yuan,[1] and Fang Lu[1,†]
[1]*Surface Physics Laboratory, Fudan University, Shanghai, China*
[2]*Department of Theoretical Physics, Research School of Physical Sciences & Engineering, Australian National University, Canberra, Australian Capital Territory 0200, Australia*
[3]*Institute of Solid State Physics, Chinese Academy of Sciences, Hefei 230031, China*
(Received 3 January 2006; revised manuscript received 13 February 2006; published 27 March 2006)

We present a combined experimental and theoretical study on the admittance spectroscopy of $Si/Si_{1-x}Ge_x/Si$ single quantum well structures. Experimentally, the admittance spectra are measured for $Si_{1-x}Ge_x$-based two-dimensional hole gas systems. The dependence of the spectra on width of the quantum well and on content of Ge is investigated. Theoretically, in conjunction with the measurements we develop a simple and systematic approach to calculate the conductance and capacitance on the basis of a Boltzmann equation in which the emission rate induced by hole-phonon scattering is considered. We compare the theoretical results with those obtained experimentally and find that our model calculation can reproduce nicely the experimental findings.

DOI: 10.1103/PhysRevB.73.125341 PACS number(s): 72.80.Cw, 72.20.Dp, 73.61.Cw

I. INTRODUCTION

The admittance spectroscopy is a powerful tool for electrical characterization of semiconductor nanostructures such as quantum wells, quantum wires, quantum dots, superlattices, etc. Using this simple technique, the important electronic properties (such as the activation energy of the carriers, the strength of the confining potential, the energy level structure, emission and capture rates, etc.) can be determined via conventional electrical measurements.[1] Since the 1990's, the admittance spectroscopy has been successfully applied in the investigation into $Si/Si_{1-x}Ge_x/Si$-based quantum well and quantum dot systems.[2–4] It is known that in these novel semiconductor structures, the conducting carriers come mainly from holes. Because the emission and capture rates of the heavy and light holes in these devices are of the order of MHz, the capacitance and conductance spectra can be observed clearly at relatively high temperatures under the action of the MHz ac electric fields. Through examining and analyzing these spectrum structures, important electronic coefficients can be obtained and determined.[2–4]

It has been found experimentally that in $Si_{1-x}Ge_x$-based quantum well structures, the capacitance and conductance spectra depend strongly on x the content of Ge and on width of the quantum well. This is due to the fact that these sample parameters relate directly to the strength of the confining potential to a two-dimensional hole gas (2DHG).[4] On the basis that the admittance spectroscopy in the quantum well systems is mainly induced by transition of conducting carriers from bound states in the well to continuum states of the system, the quantum confinement along the growth-direction plays an essential role in affecting the profile and features of capacitance and conductance along this direction. Although the dependence of the capacitance and vertical conductance in $Si/Si_{1-x}Ge_x/Si$ quantum well structures on Ge content and on width of the well layer was noticed in our previous experimental work,[4] a detailed experimental study on these important effects has not yet been well documented. In this paper, we intend examining experimentally how the admittance spectroscopy depends on these sample parameters.

At present, one of the most popularly used theoretical models in analyzing and understanding the experimental findings from the admittance spectroscopy measurements is the thermal emission model.[4] It should be noted that although the thermal emission model can give satisfactory explanations to deep level transient spectroscopy (DLTS), capacitance-voltage (C-V) features, and admittance spectroscopy for different quantum well systems, the model itself has some drawbacks. First, the model is based on a phenomenological theory which introduces the average thermal velocity of carriers in the barrier for the evaluation of the thermal emission and capture rates.[3,5] Because the carriers in the quantum well are confined, the average thermal velocity of the carriers differs from those in the bulk case, especially for the narrow quantum well structures where a stronger confinement is achieved. Secondly, the previous calculation of the thermal emission rate needs to introduce some fitting parameters,[6,7] such as the emission and capture cross sections which were often taken as input parameters. Thirdly, many results used in the thermal emission model come from those obtained for III-V quantum well structures,[2–4,7] not from $Si/Si_{1-x}Ge_x/Si$ quantum wells which we are interested in the present work. As one knows, the conducting carriers in a $Si_{1-x}Ge_x$ quantum well system are mainly holes, in contrast to a III-V quantum well in which the conducting carriers are normally electrons. Moreover, the valence-band offset in a $Si/Si_{1-x}Ge_x$ heterojunction is relatively small in comparison to the conduction-band discontinuity in an AlGaAs/GaAs heterostructure. Together with the fact that the $Si/Si_{1-x}Ge_x$ quantum well systems are normally with weak background doping, in contrast to modulation doping in an AlGaAs/GaAs-based quantum well, the hole-phonon scattering can play an important role in the emission and capture of holes in Si/SiGe-based 2DHG systems.[8,9] So far the effect of hole-phonon interaction on admittance spectroscopy in Si/SiGe-based quantum wells has not yet been taken into consideration in the thermal emission model. From a theoretical point of view, it is important and significant to be able to develop a tractable and systematic approach for the study

TABLE I. Sample parameters.

Sample No.	Well composi. x	Well thickness (nm)	Buffer thickness (nm)	Cap thickness (nm)
a	0.25	15	600	600
b	0.33	15	500	200
c	0.40	15	300	300
d	0.33	3.5	300	700

of the admittance spectroscopy in conjunction with the experimental measurements. This is one of the prime motivations of the present study. In this work, we propose to use time-dependent Boltzmann equation for the calculation of the conductance and capacitance in Si/SiGe-based quantum well structures. By employing the Boltzmann-equation approach, almost all possible scattering mechanisms can be in principle included and the emission and capture rates can be evaluated using known sample and material parameters. Thus, we can go beyond the thermal emission model and improve greatly the model calculations.

This paper is organized as follows. In Sec. II, the details of the sample devices, experimental setup and measurements are described. The theoretical approach is developed in Sec. III, where the analytical results for conductance and capacitance are presented and the results for emission rate induced by hole-acoustic-phonon scattering are obtained. The experimental and theoretical results are presented and discussed in Sec. IV and our concluding remarks are summarized in Sec. V.

II. EXPERIMENTAL MEASUREMENT

In the experimental part of the work, we measure the admittance spectra for $Si/Si_{1-x}Ge_x/Si$-based single quantum well structures. The samples are prepared using molecular beam epitaxy (MBE). The quantum well structures are grown on *p*-type Si (100) substrate (with a resistivity about 0.05 Ω cm) doped by boron with a concentration $\sim 10^{16}$ cm^{-3} at a temperature 500 °C. The samples contain three epitaxial layers (see Table I): a Si buffer layer on the Si substrate, a $Si_{1-x}Ge_x$ well layer which is narrow enough to form the quantum confinement to holes along the growth direction, and a Si cap layer. In order to observe the dependence of the admittance spectra on content of Ge in the well layer, samples a–c are with the same width of the well layer but with different Ge contents x. To see the influence of the width of the quantum wells, samples b and d are with the same x but different well thicknesses. The $Si_{1-x}Ge_x$ alloy layers in the structures are formed by coevaporating Si and Ge sources with two electron-beam evaporators. During the sample growth, the layer thickness and Ge content x are monitored *in situ* by two quartz thickness monitors within our MBE system. The width of the well layer is controlled well below the critical thickness of the pseudomorphic growth. Through the capacitance-voltage measurements, we find that the areal density of the holes in the quantum well is of the order of 10^{10} cm^{-2}. The main reason for relatively low hole densities in our samples is that in these quantum well structures, the conducting holes come mainly from ionized dopants due to background doping in the well and barrier layers. Basically, the 2D hole density depends not only on the height of the barrier but also on the Fermi level in the well. Because the doping concentration is low (about 10^{16} cm^{-3}), the Fermi level is far away from the bottom of the valance band of the well layer and, consequently, the 2D hole density in the well is relatively low.

The devices are fabricated with Schottky diode structures where an Al electrode with a diameter of 1 mm without alloying is placed at the front side and an ohmic contact is at the back side. The conductance and capacitance are measured under an ac electric field at a frequency of $f=1$ MHz, using a HP 4284A LCR meter which can also provide a dc bias voltage. The measurements are carried out at temperatures ranging from 80 to 250 K, using a thermocouple with a Keithley 2400 sourcemeter as the voltage indicator. Both meters were controlled by the computer system through the IEEE-488 interfaces. The experimental results are presented in the upper panels in Figs. 1 and 2 in Sec. IV. We note that the experimental curves in Figs. 1 and 2 are original data. As one knows, the admittance spectroscopy is a well established technique from which the good signals of the measurement can be obtained, especially when the frequency of the ac field is at $f \sim 1$ MHz.[10]

III. THEORETICAL APPROACH

A. Conductance and capacitance

In the present work, we consider a two-dimensional hole gas (2DHG) system in which the growth-direction is taken along the z axis and the 2DHG is formed along the xy plane. In conjunction with the experimental setup and measurement, we consider further the following facts and consequences. (1) A dc bias voltage and an ac electric field are applied along the growth direction of the 2DHG to measure the capacitance and conductance. The dc bias plays mainly a role in varying the hole subband structure in the well and the ac field can be taken as a driving field which alters the number of holes in the quantum well. (2) The admittance spectroscopy is mainly induced by the change of number of holes in the quantum well due to the presence of the ac driving field. (3) The changes of the hole numbers in the quantum well are mainly due to the transitions of holes from quantum well states (2D) to continuum states (i.e., hole emission) or

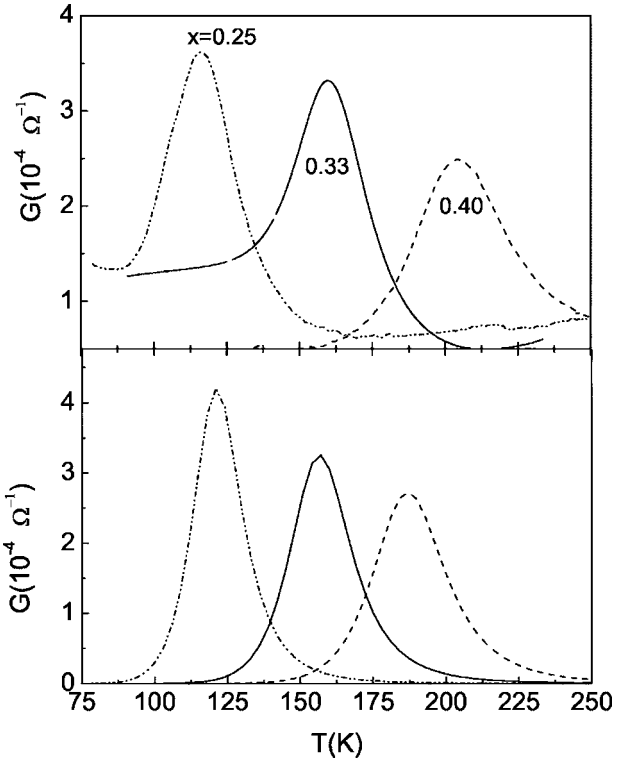

FIG. 1. Conductance G as a function of temperature T at a fixed width of quantum well $L=15$ nm for different Ge compositions x as indicated. The results are obtained under an ac electric field with a frequency $f=\omega/2\pi=1$ MHz. The experimental and theoretical results are presented, respectively, in the upper and lower panels.

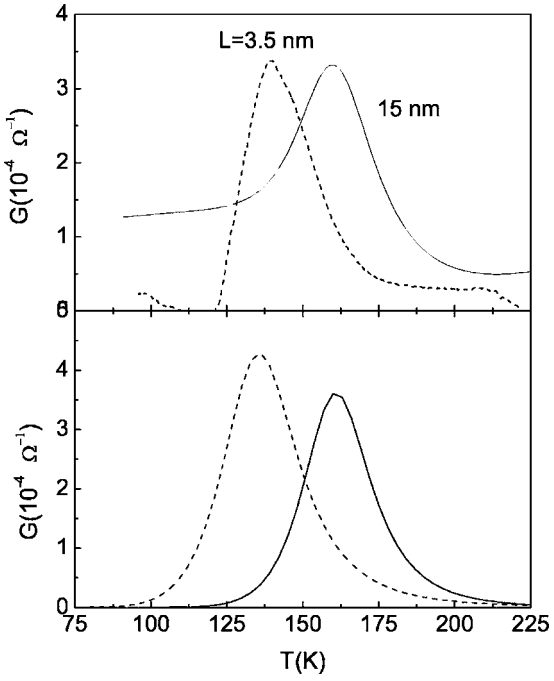

FIG. 2. Dependence of conductance on temperature at a fixed Ge content $x=0.33$ for different width of quantum wells L as indicated. The results are obtained at an ac field with a frequency $f=\omega/2\pi=1$ MHz and the upper and lower panels are, respectively, for experimental and theoretical results.

from continuum states (3D) to bound-states in the quantum well (i.e., hole capture). (4) The transition of holes among different states is a consequence of the presence of the ac field and of the electronic scattering mechanisms. Taking these points into consideration, we can employ the semiclassic Boltzmann equation as the governing transport equation to calculate the admittance spectroscopy. Because the ac field is a time-dependent field and our measurements are carried out at relatively high temperatures for relatively low-carrier-density samples, we start our calculation from a time-dependent Boltzmann equation in nondegenearte statistics. For 3D and 2D holes, we, respectively, have

$$\frac{\partial f_{3D}(\mathbf{K};t)}{\partial t} = g_s \sum_{n',\mathbf{k}'} [f_{2D}(n',\mathbf{k}';t) W_{2D\to 3D}(\mathbf{k}',n';\mathbf{K}) - f_{3D}(\mathbf{K};t) W_{3D\to 2D}(\mathbf{K};\mathbf{k}',n')] + g_s \sum_{\mathbf{K}'} [f_{3D}(\mathbf{K}';t) W_{3D\to 3D}(\mathbf{K}';\mathbf{K}) - f_{3D}(\mathbf{K};t) W_{3D\to 3D}(\mathbf{K};\mathbf{K}')] \quad (1)$$

and

$$\frac{\partial f_{2D}(n,\mathbf{k};t)}{\partial t} = g_s \sum_{\mathbf{K}'} [f_{3D}(\mathbf{K}';t) W_{3D\to 2D}(\mathbf{K}';n,\mathbf{k}) - f_{2D}(n,\mathbf{k};t) W_{2D\to 3D}(n,\mathbf{k};\mathbf{K}')] + g_s \sum_{n',\mathbf{k}'} [f_{2D}(n',\mathbf{k}';t) W_{2D\to 2D}(n',\mathbf{k}';n,\mathbf{k}) - f_{2D}(n,\mathbf{k};t) W_{2D\to 2D}(n,\mathbf{k};n',\mathbf{k}')]. \quad (2)$$

Here, $|n,\mathbf{k}\rangle$ and $|\mathbf{K}\rangle$ are, respectively, the states for 2D and 3D holes with $\mathbf{K}=(\mathbf{k},k_z)=(k_x,k_y,k_z)$ being the hole wave vector and n the index for the nth hole subband in the quantum well, $f_{2D}(n,\mathbf{k};t)$ and $f_{3D}(\mathbf{K};t)$ are, respectively, the momentum-distribution functions for 2D and 3D holes, $g_s=2$ counts for spin degeneracy, and $W_{\alpha\to\beta}(\mathcal{A};\mathcal{B})$ is the electronic transition rate for scattering of a hole from $\mathcal{A}$ state in α to $\mathcal{B}$ state in β. In Eqs. (1) and (2), the effect of scattering centers is included within the electronic transition rate, the effect of the dc bias can be included within the hole wave function and energy spectrum, and the effect of the ac field can be included within time-dependent hole distribution functions. Thus, to avoid double counting, the force terms induced by the dc and ac fields do not appear on the left-hand side of the Boltzmann equation. It is known that there is no simple and analytical solution to Eqs. (1) and (2). In this work, we apply the usual balance-equation approach to solve the problem.[11] For the first moment, the mass-balance equation (or rate equation)[12] can be derived by multiplying $\Sigma_{\mathbf{K}}$ and $\Sigma_{n,\mathbf{k}}$, respectively, to both sides of Eqs. (1) and (2). In doing so, we obtain two rate equations

$$\frac{dQ_{3D}(t)}{dt} = Q_{2D}(t)\lambda_{2D\to 3D} - Q_{3D}(t)\lambda_{3D\to 2D} \tag{3}$$

and

$$\frac{dQ_{2D}(t)}{dt} = Q_{3D}(t)\lambda_{3D\to 2D} - Q_{2D}(t)\lambda_{2D\to 3D}, \tag{4}$$

where Q_{2D} and Q_{3D} are, respectively, the charge numbers for 2D and 3D holes and $\lambda_{\alpha\to\beta}$ is the scattering rate from a state α to a state β. We have used the definition that the 2D and 3D hole densities are, respectively, $N_{2D}(t) = g_s\Sigma_{n,\mathbf{k}} f_{2D}(n,\mathbf{k};t)$ and $N_{3D}(t) = g_s\Sigma_{\mathbf{K}} f_{3D}(\mathbf{K};t)$ and $Q_{2D}(t) = eN_{2D}(t)S$ and $Q_{3D}(t) = eN_{3D}(t)SL_z$, with S being the area of the 2D plane and L_z the size of the z direction. Equations (3) and (4) give a condition of total hole number conservation $d[Q_{2D}(t)+Q_{3D}(t)]/dt = 0$ and reflect a fact that the 2D→2D and 3D→3D transitions do not contribute to the change of hole numbers in the quantum well and in the continuum states. Furthermore, $\lambda_{2D\to 3D} = \lambda_E$ is the emission rate and $\lambda_{3D\to 2D} = \lambda_C$ is the capture rate, which are

$$\lambda_E = \frac{2}{N_{2D}} \sum_{n,\mathbf{k},\mathbf{K}'} f_{2D}(n,\mathbf{k};t) W_{2D\to 3D}(n,\mathbf{k};\mathbf{K}'), \tag{5}$$

and

$$\lambda_C = \frac{2}{L_z N_{3D}} \sum_{n',\mathbf{k}',\mathbf{K}} f_{3D}(\mathbf{K};t) W_{3D\to 2D}(\mathbf{K};n',\mathbf{k}'). \tag{6}$$

In the calculation of the emission and capture rates under the condition of a weak ac field, we can neglect the influence of the ac field on the momentum distribution function and employ the statistical energy distribution as hole distribution function. We take $f_{2D}(n,\mathbf{k};t) \simeq f[E_n(\mathbf{k})]$ and $f_{3D}(\mathbf{K};t) \simeq f[E(\mathbf{K})]$ with $f(x)$ being an energy distribution function. Here, $E_n(\mathbf{k}) = \hbar^2k^2/2m^* + \varepsilon_n$ and $E(\mathbf{K}) = \hbar^2K^2/2m^* + U_0$ are, respectively, the energy spectra for 2D and 3D holes, where m^* is the hole effective-mass, ε_n is the energy of the nth hole subband in the quantum well, and U_0 is the height of the barrier to the quantum well. Thus, the emission and capture rates become

$$\lambda_E \simeq \frac{2}{N_{2D}} \sum_{n,\mathbf{k},\mathbf{K}'} f[E_n(\mathbf{k})] W_{2D\to 3D}(n,\mathbf{k};\mathbf{K}') \tag{7}$$

and

$$\lambda_C \simeq \frac{2}{L_z N_{3D}} \sum_{n,\mathbf{k},\mathbf{K}'} f_{3D}[E(\mathbf{K})] W_{3D\to 2D}(\mathbf{K}';n,\mathbf{k}), \tag{8}$$

which are time independent when taking N_{2D} and N_{3D} as their values at the steady state.

Using Eq. (4), the current in the circuit is given by

$$I(t) = -\frac{dQ_{2D}(t)}{dt} = Q_{2D}(t)\lambda_E - Q_{3D}(t)\lambda_C. \tag{9}$$

It is known that under the action of an ac driving field $\delta V_t = V_0 e^{i\omega t}$ with ω being the frequency of the field, the hole number in the quantum well $Q_{2D}(t)$ is the difference between the mobil hole number $\delta Q_{2D}(t)$ and the emitted hole number $\int_0^t dt\, I(t)$, namely,

$$Q_{2D}(t) = \delta Q_{2D}(t) - \int_0^t dt I(t). \tag{10}$$

For case of a weak ac field so that a linear response is achieved, we have

$$\delta Q_{2D}(t) = \kappa \delta V_t = \kappa V_0 e^{i\omega t} \text{ and } I(t) = I_0 e^{i\omega t}. \tag{11}$$

Here a coefficient $\kappa = \delta Q_{2D}(t)/\delta V_t = dQ_{2D}(t)/dV_t$ (see Appendix) is introduced. Inserting Eqs. (10) and (11) into Eq. (9), we get

$$I(t) = \left(\kappa V_0 e^{i\omega t} - \int_0^t I(t)dt\right)\lambda_E - Q_{3D}(t)\lambda_C$$

and, as a result,

$$\dot{I}(t) = [i\omega\kappa V_0 e^{i\omega t} - I(t)]\lambda_E - \dot{Q}_{3D}(t)\lambda_C. \tag{12}$$

When the system is in equilibrium, the total charge number should be conserved so that $\dot{Q}_{3D}(t) = -\dot{Q}_{2D}(t) = I(t)$. Thus, Eq. (12) can be solved analytically. After using the definitions for conductance $\mathcal{G} = I_0/V_0$ and for capacitance $\mathcal{C} = -dQ_{2D}(t)/dV_t = -[dQ_{2D}(t)/dt]/[dV_t/dt]$, we obtain

$$\mathcal{G} = \frac{i\kappa\omega\lambda_E}{\lambda_E + \lambda_C + i\omega} \text{ and } G = \text{Re}\,\mathcal{G} = \frac{\kappa\omega^2\lambda_E}{(\lambda_E+\lambda_C)^2 + \omega^2}, \tag{13}$$

and

$$\mathcal{C} = \frac{\kappa\lambda_E}{\lambda_E + \lambda_C + i\omega} \text{ and } C = \text{Re}\,\mathcal{C} = \frac{\kappa\lambda_E(\lambda_E+\lambda_C)}{(\lambda_E+\lambda_C)^2 + \omega^2}. \tag{14}$$

In contrast to the results obtained from thermal emission model, the capture rate λ_C appears in both conductance and capacitance when the balance-equation approach is employed on the basis of a Boltzmann equation. As one can see, Eqs. (13) and (14) become those used popularly when $\lambda_E \gg \lambda_c$.

B. Emission rate

From now on, we consider $Si/Si_{1-x}Ge_x$-based 2DHG systems. For low-carrier-density samples, only the heavy-hole states in the quantum well are occupied. Due to the higher energy levels for light holes in the quantum well, the contributions to the conductance and capacitance from light holes are relatively small. We therefore take only the heavy holes into account in the present study. For samples with weak background doping and at relatively high temperatures, the hole-phonon scattering is the principle channel for relaxation of excited holes. Furthermore, it is known that in $Si_{1-x}Ge_x$-based 2DHG, the hole-phonon scattering comes mainly from interactions with acoustic-phonons via deformation potential coupling.[8,13] The electronic transition rate induced by hole–acoustic-phonon coupling in a 2DHG system can be obtained from Fermi's golden rule,[14,15] which reads

$$W_{2D\to 3D}(n,\mathbf{k};\mathbf{K}') = \frac{2\pi}{\hbar}|U_{\mathbf{Q}}|^2\left[N_Q + \frac{1}{2} \mp \frac{1}{2}\right] \times R(k_z',n;q_z)\delta_{\mathbf{k}',\mathbf{k}+\mathbf{q}}\delta[E(\mathbf{K}') - E_n(\mathbf{k}) \pm \hbar\omega_Q] \quad (15)$$

and

$$W_{3D\to 2D}(\mathbf{K};n',\mathbf{k}') = \frac{2\pi}{\hbar}|U_{\mathbf{Q}}|^2\left[N_Q + \frac{1}{2} \mp \frac{1}{2}\right] \times R(k_z,n';q_z)\delta_{\mathbf{k}',\mathbf{k}+\mathbf{q}}\delta[E_{n'}(\mathbf{k}') - E(\mathbf{K}) \pm \hbar\omega_Q]. \quad (16)$$

Here, the upper (lower) case refers to phonon absorption (emission), $\mathbf{Q}=(\mathbf{q},q_z)=(q_x,q_y,q_z)$ is the phonon wave vector, ω_Q is the acoustic-phonon frequency, $N_Q=[e^{\hbar\omega_Q/k_BT}-1]^{-1}$ is the phonon occupation number, and $R(k_z',n;q_z)=|\langle k_z'|e^{iq_zz}|n\rangle|^2$ is the form factor for hole-phonon coupling in a 2D system with $|k_z\rangle=e^{ik_zz}$ and $|n\rangle=\psi_n(z)$ being, respectively, the 3D and 2D hole wave function along the z direction. Moreover, $|U_{\mathbf{Q}}|^2=(\hbar Q/2\rho)(\Xi_L^2/u_L+\Xi_T^2/u_T)$ is the square of the hole–acoustic-phonon interaction matrix for intravalley scattering via deformation potential coupling,[16] where ρ is the density of the material, u_L and u_T are, respectively, the longitudinal and transverse sound velocities, $\Xi_L=\Xi_d+\Xi_u\cos^2\theta$ and $\Xi_T=\Xi_u\cos\theta\sin\theta$ with Ξ_d and Ξ_u being, respectively, the dilatation and uniaxial deformation potential constants and θ an angle to the z axis. Here we have included the contributions from both longitudinal and transverse acoustic-phonon coupling and $\omega_Q=u_LQ$ or $\omega_Q=u_TQ$ is the corresponding phonon frequency.

At relatively high-temperatures and for relatively low-carrier-density samples, we can use Maxwellian as statistic energy-distribution function for holes, i.e., $f(x)=Ce^{-x/k_BT}$. The normalization factors C for 2D and 3D holes can be determined by definition $N_{2D}=g_s\Sigma_{n,\mathbf{k}}f[E_n(\mathbf{k})]$ and $N_{3D}=g_s\Sigma_{\mathbf{K}}f[E(\mathbf{K})]$, which give

$$C_{2D}=\frac{\pi\hbar^2N_{2D}}{m^*k_BTA_{2D}} \text{ and } C_{3D}=\left(\frac{2\pi\hbar^2}{m^*k_BT}\right)^{3/2}\frac{N_{3D}}{2A_{3D}},$$

where $A_{2D}=\Sigma_n e^{-\varepsilon_n/k_BT}$ and $A_{3D}=e^{-U_0/k_BT}$. It should be noted that in a single quantum well, the 3D holes are located in both well and barrier layers. Due to the higher energy levels for 3D holes in the well layer, the 3D hole density in the well layer is very low in comparison to the 2D hole density N_{2D}. For a real working device, the edges of the valance band is bent by the the presence of the Hartree potential induced by hole-hole interaction.[20] The obtained theoretical results indicate that for a Si/SiGe/Si single quantum well, the bending of the valence band in the barrier layers can reach up to the half-height of the quantum well.[20] Thus, the transition from 3D hole states in the barrier layers to the 2D states in the quantum well needs to across the barrier induced by the Hartree potential (which is a tunneling process). Because the 2D holes are confined within the quantum well, the coupling of the wave functions for a 2D hole and for a 3D hole in the barrier layer is very weak. Hence, the tunneling rate from a 3D state in the barrier layer to a 2D state in the well is very low. For the same reason, the tunneling from a 2D state in the well to a 3D state in the barrier can also be neglected. As a result, under the action of the ac fields, the emission rate induced by hole-phonon scattering is much larger than the capture rate, i.e., $\lambda_E \gg \lambda_C$. Based on these reasons, in the present study we neglect the contribution from tunneling processes and from λ_C and we consider only λ_E caused by hole-phonon interaction in Eqs. (13) and (14). At relatively high temperatures, the acoustic-phonon energy $\hbar\omega_Q$ is much smaller than the thermal energy k_BT. When $\hbar\omega_Q/k_BT \ll 1$ we can use the usual approximation for acoustic-phonon occupation number[13] $N_Q \sim N_Q+1 \simeq k_BT/\hbar\omega_Q$. The emission rate is now given as

$$\lambda_E \simeq \frac{\sqrt{\pi k_BT}}{2\pi\hbar^2A_{2D}}\sum_{n,\mathbf{Q}}\frac{|U_{\mathbf{Q}}|^2}{\omega_Q\sqrt{E_q}}e^{-\varepsilon_n/k_BT}\int_{-\infty}^{\infty}dk_z \times e^{-(E_{k_z}+E_q+U_0-\varepsilon_n\pm\hbar\omega_Q)^2/(4E_qk_BT)}R(k_z,n;q_z), \quad (17)$$

where $E_{k_z}=\hbar^2k_z^2/2m^*$ and $E_q=\hbar^2q^2/2m^*$. Due to the usage of the Maxwellian as the hole distribution function, λ_E does not depend directly to the density of holes.

To simplify the analytical and numerical calculations, in this work we neglect the strain effects in a SiGe quantum well via considering an ideal 2DHG system in which conducting carriers are mainly heavy holes in a parabolic band structure. We take the usual square-well approximation to model the confining potential along the growth direction. In doing so, we have

$$\psi_n(z)=(2/L)^{1/2}\sin(n\pi z/L) \quad (18)$$

and

$$\varepsilon_n=n^2\pi^2\varepsilon_0, \quad (19)$$

with L being the width of the quantum well and $\varepsilon_0=\hbar^2/(2m^*L^2)$. This approximation also implies that the coupling between the 2D holes in the well layer and the 3D holes in the barrier layer has been neglected. Thus, the form factor for hole-phonon coupling for 2D and 3D holes in the well layer can be obtained analytically $R(k_z,n;q_z)=4LS_n[(k_z+q_z)L]$ and

$$S_n(x)=(n\pi)^2\frac{1-(-1)^n\cos x}{[(n\pi)^2-x^2]^2}.$$

Here we mainly consider the case of a weak dc bias applied to the device so that the effect of bending of the valence band is negligible. For case of a strong bias, the profile of the confining potential along the z direction can be determined self-consistently by solving coupled Schrödinger and Poisson equations.[17] Finally, the emission rate induced by hole–acoustic-phonon scattering is obtained as

TABLE II. Material parameters (Ref. 9, 18, and 19).

quantity	symbol	value	unit
Longitudinal sound velocity	u_L	5247	m/s
Transverse sound velocity	u_T	3267	m/s
Dilatation deformation potential (Ge)	Ξ_d	2.0	eV
Uniaxial deformation potential (Ge)	Ξ_u	−2.16	eV
Density (Ge)	ρ	5.323	g/cm^3

$$\lambda_E = \frac{\sqrt{2\pi m^* k_B T}\Xi_d^2}{4\pi^3\hbar^2\rho u_L^2 L^2 A_{2D}} \sum_n e^{-\pi^2 n^2 \beta_0} \int_{-\infty}^{\infty} dx S_n(x) \int_0^{\infty} dy \times \int_{-\infty}^{\infty} dz \left[\left(1 + \frac{\Xi_u}{\Xi_d}\cos^2\theta\right)^2 + \left(\frac{\Xi_u u_L}{\Xi_d u_T}\right)^2 \cos^2\theta \sin^2\theta \right] \times e^{-[(x-z)^2 + y^2 + U_0/\varepsilon_0 - \pi^2 n^2 \pm \hbar\omega_Q/\varepsilon_0]^2 \beta_0/4y^2}, \quad (20)$$

where $\cos\theta = z/\sqrt{y^2+z^2}$, $\sin\theta = y/\sqrt{y^2+z^2}$, $Q = \sqrt{y^2+z^2}/L$, and $\beta_0 = \varepsilon_0/k_B T$.

C. Si/Si$_{1-x}$Ge$_x$/Si quantum wells

It is known that a strained SiGe quantum well is under compression in some cases, which may cause some alterations to the valance-band structure. As a result, the valance-bands may no longer be designed as heavy and light holes bands (due to the lifting of the degeneracy at the Γ point) and the valence-band maxima become anisotropic so that the hole effective-mass differs along different crystal axes. To look into these effects, a detailed band-structure calculation (e.g., using a $\mathbf{k}\cdot\mathbf{p}$ approach) is needed, which requires a further analytical and numerical considerably. In the present work, we do not attempt these band-structure calculations and we consider a rather ideal case (i.e., the heavy and light holes are well separated and the system is isotropic) which is popularly applied in simplified theoretical calculations. For Si/Si$_{1-x}$Ge$_x$/Si quantum well systems, the effective-mass for heavy and light holes in the well layer and the valance-band offset at the heterointerfaces are in general the functional form of the Ge content x. Here we use the well known and popularly used results[19] to evaluate these material parameters. For heavy (h) and light (l) holes, the corresponding effect masses are[19]

$$\begin{bmatrix} m_h \\ m_l \end{bmatrix} / m_0 = \begin{bmatrix} -2.8369 \\ -0.1432 \end{bmatrix} x^3 + \begin{bmatrix} 4.6844 \\ 0.3618 \end{bmatrix} x^2 + \begin{bmatrix} -2.8700 \\ -0.3669 \end{bmatrix} x + \begin{bmatrix} 0.8956 \\ 0.2534 \end{bmatrix}.$$

The valence-band offset at the Si/Si$_{1-x}$Ge$_x$ interface is[19] $\Delta E_v = U_0 = 0.71x$ eV. Other parameters taken in the calculation are well known and are listed in Table II.

In the numerical calculations, we take the high-temperature and low-carrier-density result for the coefficient κ (see the Appendix)

$$\kappa \simeq \frac{N_{2D} e^2 S}{k_B T}.$$

The 2D hole density is taken from the experimental data $N_{2D} \simeq 10^{10}$ cm^{-2} and the area of the sample in the xy plane is $S \simeq 1$ mm^2. The admittance spectrum is calculated through

$$G \simeq \frac{\kappa\omega^2\lambda_E}{\lambda_E^2 + \omega^2}.$$

IV. RESULTS AND DISCUSSIONS

The dependence of the vertical conductance G on Ge composition x and on width of quantum well L is shown, respectively, in Figs. 1 and 2. Here we plot G as a function of temperature at a fixed ac electric field with a frequency $f = \omega/2\pi = 1$ MHz. As we know, with increasing Ge content x in the well layer with a fixed well width, a larger valence band offset can be achieved so that a stronger confinement of the 2DHG can be realized. In such a case, the holes in the quantum well are more difficult to be emitted by the action of the ac field and by the corresponding scattering mechanisms. This corresponds to a smaller emission rate and, as a result, the peak of the ac conductance shifts to the higher-temperature regime. With increasing x, the height of the conductance peak decreases, which can be found from both experimental and theoretical results shown in Fig. 1. On the other hand, with decreasing width of the quantum well L at a fixed Ge content (i.e., a fixed height of the confinement potential), the hole subbands in the well are pushed higher [see Eq. (19)]. This implies that the energy distance between the bound states in the well and the continuum states is shorter for a narrower quantum well. In such a case, the holes in the quantum well are much easier to be emitted than those in the wider quantum well. Thus, a larger emission rate can be achieved in a narrower quantum well and, consequently, the peak of the ac conductance in a narrower well is shifted to the lower-temperature regime. We see these interesting features clearly from both experimental and theoretical results shown in Figs. 1 and 2.

The results shown in Figs. 1 and 2 are obtained for the case of a weak dc bias applied to the system. The experimental results on how a dc bias affects the conductance spectra can be found in our previous work.[21] Because the effect of the dc bias has not been included within the hole wave function and energy spectrum in Eqs. (18) and (19), the square-well approximation used here cannot be employed to handle such a case.

From a theoretical point of view, the hole-phonon interaction affects strongly the emission rate in shallow and/or narrow quantum well structures. In such a case, the holes can gain the energy from the ac field and loss the energy by emission and absorption of phonons. Due to inelastic nature of the hole-phonon scattering and to the fact that hole-phonon scattering can alter the hole wave vector (or momen-

tum) efficiently, this process can be accompanied by transition of the holes from the bound states in the well to the continuum states in the system. It can be seen from Figs. 1 and 2 that the results obtained from our theoretical calculation are in good agreement with those measured experimentally. The theoretical calculation can reproduce the dependence of the ac conductance on both Ge content and width of the well layer, especially the peak structure observed experimentally. For example, we find that when $x=0.33$ and $L=15$ nm, theoretically the peak position is at about 157 K and the half-width of the peak is about 27 K, in comparison to a peak position at 160 K and half-width of the peak being at 30 K obtained experimentally. These results indicate that the hole-phonon scattering plays an important role in affecting the emission rate in Si/SiGe quantum well systems, which can describe rightly the dependence of the ac conductance on experimental conditions and sample parameters.

From Figs. 1 and 2 we note that there are some minor differences between the experimental and theoretical results. The calculated conductance is slightly larger than measured data. We believe that this mainly results from taking the larger deformation potential constants Ξ_d and Ξ_u. The Ξ_d and Ξ_u shown in Table II are for bulk Ge material and they should be slightly less for SiGe compound. More markedly, the disagreement between the experimental and theoretical results can be found for conductance off the peak, mainly at low temperatures. As was observed previously,[20] in the measurement there exists the variations of the leakage current on Schottky contact and of the Schottky capacitance at low temperatures. These variations have not been included within the calculation. It should be pointed out that in using the admittance spectroscopy for characterization of semiconductor nanostructures, we mainly examine and analyze the data near the peak of the conductance and/or capacitance. Hence, the disagreement of the off-peak experimental and theoretical results does not affect on using the current model calculation to analyze and understand the experimental findings.

We have also included the light holes within the numerical calculations and found that, due to the higher energy levels for the light-hole subbands, the contribution of light holes to the ac conductance is rather small under the current experimental conditions. Thus, our theoretical results confirm that heavy-holes are responsible for the admittance spectroscopy observed at $T\sim 100$ K and $f\sim 1$ MHz.

V. SUMMARY AND CONCLUSIONS

In this work, we have carried out a combined experimental and theoretical study on admittance spectroscopy in $Si/Si_{1-x}Ge_x/Si$ single quantum well systems. Experimentally, we have measured the ac conductance on series of samples in order to examine the dependence of the admittance spectroscopy on different sample growth parameters. Theoretically, we have developed a systematic and tractable approach to calculate the conductance and capacitance under the action of an ac field, in conjunction with the experiments and experimental findings. The main conclusions obtained from this work are summarized as follows.

We have found experimentally that for samples with higher Ge content and/or wider width of the well layer, the peaks of the ac conductance shift to the higher-temperature regime. This effect is mainly resulted from the fact that higher Ge composition in a Si/SiGe quantum well corresponds to a stronger confinement of the 2DHG in the well and that a wider width of well leads to lower the hole subband energies. In such cases, it is harder for holes in the quantum well to be emitted to the continuum states in the systems. We also found that with increasing Ge content and/or width of quantum well, the height of the conductance peak decreases.

We have developed a simple theoretical approach to calculate the conductance and capacitance under an ac electric field in two-dimensional systems, in conjunction with the admittance spectroscopy measurements. The theory is based on applying the balance-equation approach to the time-dependent Boltzmann equation. Using this approach, the emission and capture rates in a quantum well can be calculated from microscopic quantum-mechanical theories and the drawbacks of popularly used thermal emission model can be overcome. We have calculated the emission rate induced by hole-acoustic-phonon interaction via deformation potential coupling in $Si/Si_{1-x}Ge_x$-based 2DHG systems. The theoretical results are in good agreement with those obtained experimentally, especially the peak structure of the spectra. Although some more complicated sample details (e.g., strain and anisotropic effects and the presence of a strong dc gate voltage) have not been taken into account, the model calculation can reproduce nicely the experimental findings such as the dependence of the admittance spectroscopy on sample parameters and experimental conditions.

On the basis of our experimental and theoretical results, we believe that the hole-phonon scattering plays an important role in determining the emission rate and admittance spectroscopy in Si/SiGe-based low-carrier-density 2DHG systems ($N_{2D}\sim 10^{10}$ cm^{-2}) at relatively high temperatures ($T\sim 100$ K). We hope this work can shed some lights on the measurements and calculations of electronic and transport properties of Si/SiGe-based semiconductor nanostructures.

ACKNOWLEDGMENTS

This work was supported by the special funds for Major State Basic Research Project No. G2001CB3095 of China, the National Natural Science Foundation of China, and by the Commission of Science and Technology of Shanghai City. One of us (W.X.) was supported by the Australian Research Council via a Research Fellowship and a Linkage-International Award.

APPENDIX

In this appendix, we evaluate a coefficient defined as $\kappa = dQ_{2D}(t)/dV_t$ in Eq. (11). By definition, $Q_{2D}(t)=eSN_{2D}(t) = eSg_s\Sigma_{n,\mathbf{k}}f[E_n(\mathbf{k})]$, where $f(x)=[e^{(x-\mu_t)/k_BT}+1]^{-1}$ is the Fermi-Dirac function with μ_t being the chemical potential (or Fermi energy). Here we assume that the effect of the ac driving field is mainly on the Fermi energy of the system. Thus,

$$\kappa = 2eS\sum_{n,\mathbf{k}} \frac{\partial f[E_n(\mathbf{k})]}{\partial \mu_t} \frac{\partial \mu_t}{\partial V_t}. \tag{A1}$$

Noting that for a weak ac field so that a linear response is achieved, we have

$$\frac{1}{e}\frac{\partial \mu_t}{\partial V_t} = 1. \tag{A2}$$

Consequently,

$$\kappa = \frac{2e^2S}{k_BT}\sum_{n,\mathbf{k}} f[E_n(\mathbf{k})]\{1 - f[E_n(\mathbf{k})]\}. \tag{A3}$$

This result reflects a fact that the emission and capture of holes are mainly achieved for transitions around the Fermi level. The result is also in line with that obtained by Chang and co-workers.[22] At high temperatures and for low-carrier-density samples, $N_{2D}/k_BT \ll 1$ and, as a result,

$$\kappa \simeq \frac{N_{2D}e^2S}{k_BT}, \tag{A4}$$

which depends on temperature and density of 2D holes.

*Electronic address: wen105@rsphysse.anu.edu.au
†Electronic address: fanglu@fudan.edu.cn

[1] G. Vincent, D. Bois, and P. Pinard, J. Appl. Phys. **46**, 5173 (1975).
[2] Jian-hong Zhu, Da-wei Gong, Bo Zhang, Fang Lu, Chi Sheng, Heng-hui Sun, and Xun Wang, Phys. Rev. B **52**, 8959 (1995).
[3] K. Schmalz, I. N. Yassievich, H. Rücker, H. G. Grimmeiss, H. Frankenfeld, W. Mehr, H. J. Osten, P. Schley, and H. P. Zeindl, Phys. Rev. B **50**, 14287 (1994).
[4] Fang Lu, Jiayu Jiang, Henghui Sun, Dawei Gong, Xiangjiu Zhang, and Xun Wang, Phys. Rev. B **51**, 4213 (1995).
[5] P. A. Martin, K. Meehan, P. Gavrilovic, K. Jr. Hess, and J. J. Coleman, J. Appl. Phys. **54**, 4689 (1983).
[6] N. Debbar, Dipankar Biswas, and Pallab Bhattacharya, Phys. Rev. B **40**, 1058 (1989).
[7] Jian-hong Zhu, Da-wei Gong, Bo Zhang, Fang Lu, Chi Sheng, Heng-hui Sun, and Xun Wang, Phys. Rev. B **52**, 8959 (1995).
[8] Frank L. Madarasz, Phys. Rev. B **24**, 4611 (1981).
[9] M. V. Fischettia and S. E. Laux, J. Appl. Phys. **80**, 2234 (1996).
[10] See, e.g., K. Nauka, T. I. Kamins, J. E. Turner, C. A. King, J. L. Hoyt, and J. F. Gibbons, Appl. Phys. Lett. **60**, 195 (1992); M. Ershov, B. Yaldiz, A. G. U. Perera, S. G. Matsik, H. C. Liu, M. Buchanan, Z. R. Wasilewski, and M. D. Williams, Infrared Phys. Technol. **42**, 259 (2001).
[11] W. Xu, Phys. Rev. B **57**, 12939 (1998).
[12] T. J. Green and W. Xu, J. Appl. Phys. **88**, 3166 (2000).
[13] Carlo Jacoboni and Lino Reggiani, Rev. Mod. Phys. **55**, 645 (1983).
[14] G. D. Mahan, Phys. Rep. **145**, 251 (1987).
[15] K. Seeger, *Semiconductor Physics: An Introduction* (Springer-Verlag, Berlin, 1986).
[16] H. Mizuno, K. Taniguchi, and C. Hamaguchi, Phys. Rev. B **48**, 1512 (1993).
[17] W. Xu, Phys. Rev. B **50**, 14601 (1994).
[18] F. Schaffler, in *Properties of Advanced Semiconductor Materials: GaN, AlN, InN, BN, SiC, SiGe*, edited by M. E. Levinshtein, S. L. Rumyantsev, and M. S. Shur (Wiley, New York, 2001).
[19] Lianfeng Yang, Jeremy R. Watling, Richard C. W. Wilkins, Mirela Boric, John R. Barker, Asen Asenov, and Scott Roy, Semicond. Sci. Technol. **19**, 1174 (2004).
[20] Fang Lu, Jiayu Jiang, Henghui Sun, Dawei Gong, and Xun Wang, J. Appl. Phys. **75**, 2957 (1994).
[21] F. Lu, S. K. Zhang, Z. M. Jiang, J. Qin, D. Z. Hu, and X. Wang, J. Korean Phys. Soc. **34**, 73 (1999).
[22] W.-H. Chang, W. Y. Chen, M. C. Cheng, C. Y. Lai, T. M. Hsu, N. T. Yeh, and J. I. Chyi, Phys. Rev. B **64**, 125315 (2001).